

# Residual stress and strain in pyrolytic boron nitride resulting from thermal anisotropy

N. NAITO

*GTE Sylvania, Portsmouth Avenue, Exeter, New Hampshire 03833, USA*

C. H. HSUEH

*Metals and Ceramics Division, Oak Ridge National Laboratory, Oak Ridge, Tennessee, 37831, USA*

Residual stresses in chemically deposited pyrolytic boron nitride (PBN) crucibles caused by thermal expansion anisotropy during cooling immediately following deposition are analysed. The calculations reveal that radial tension and combined tangential tension and compression exist in the crucible. The maximum stresses increase with an increase in the thickness of the crucible. Furthermore, while the outer wall of the crucible always shrinks upon cooling, the inner wall may expand, due to the residual stress states, resulting in a negative effective thermal expansion coefficient in the tangential direction. The influence of the PBN attachment to the mandrel on which it is deposited is also considered. Specifically, the radial tensile stress in the crucible is shown to increase due to this attachment, which in turn, enhances the delamination of the crucible.

## 1. Introduction

Boron nitride crucibles are synthesized with a high-temperature and low-pressure chemical vapour deposition (CVD) technique [1-6]. The crucible is produced by depositing PBN on a mandrel having the desired configuration. When the vapour deposition is complete, the finished PBN is slipped off the mandrel [5, 7]. Articles of PBN produced by the CVD process are shown in Fig. 1. During deposition, PBN basal planes are oriented parallel to the deposition surface forming a highly oriented crystal structure consisting of laminar sheets isostructural to that of graphite. Consequently, a large degree of anisotropy exists between the planes parallel and perpendicular to the deposition surface [8-11]. Large differential thermal properties such as conductivity and expansion between directions parallel and perpendicular to the deposition surface have been measured [7, 12]. Furthermore the layered structure of PBN [13, 14] typically results in low tensile strength in the direction perpendicular to the layer (i.e. radial direction). In addition, residual radial tensile stress develops due to the higher thermal expansion coefficient in the radial direction compared to the tangential direction upon cooling. When the radial tensile stress exceeds the low radial tensile strength of the "laminates", delamination in PBN (Fig. 2) can occur and relax these stresses.

In this paper, the stress distributions within the PBN crucible due to the thermal contraction mismatch during cooling are calculated. Furthermore because attachment of the PBN crucible to the mandrel may occur during cooling, the effects of this attachment on the stresses are also considered. Finally, effective thermal expansion coefficients are defined, such that the total strains in the crucible, during cooling and constrained shrinkage, can be treated as stress-free strains.

## 2. Stress analysis

In order to analyse the problem, a two-dimensional geometry (Fig. 3) is considered in the present study with the crucible having the inner and outer radii of  $a$  and  $b$ , respectively. Furthermore, the temperature is assumed to be uniform throughout the thickness of the crucible (the typical thickness is 0.5 to 0.8 mm) during cooling. The radial and tangential stresses,  $\sigma_r$  and  $\sigma_\theta$ , satisfy the equation of equilibrium [15]

$$\frac{d\sigma_r}{dr} + \frac{\sigma_r - \sigma_\theta}{r} = 0 \quad (1)$$

The total strains  $\varepsilon_r$  and  $\varepsilon_\theta$  can be related to the stresses by [15]

$$\varepsilon_r = \frac{1}{E}(\sigma_r - \nu\sigma_\theta) + \alpha_r\Delta T \quad (2a)$$

$$\varepsilon_\theta = \frac{1}{E}(\sigma_\theta - \nu\sigma_r) + \alpha_\theta\Delta T \quad (2b)$$

where  $E$  is the Young's modulus,  $\nu$  is the Poisson ratio,  $\Delta T$  is the temperature change during cooling (negative),  $\alpha_r$  and  $\alpha_\theta$  are the thermal expansion coefficients in the radial and tangential directions, respectively. Furthermore, with  $u$  denoting the radial displacement, we have [15]

$$\varepsilon_r = \frac{du}{dr} \quad (3a)$$

$$\varepsilon_\theta = \frac{u}{r} \quad (3b)$$

Solutions of Equations 1 to 3 yield,

$$u = (1 - \nu)(\alpha_r - \alpha_\theta)\Delta T \left( \frac{r}{2} \ln \frac{r}{a} - \frac{r^2 - a^2}{4r} \right) + C_1 r + \frac{C_2}{r} \quad (4a)$$

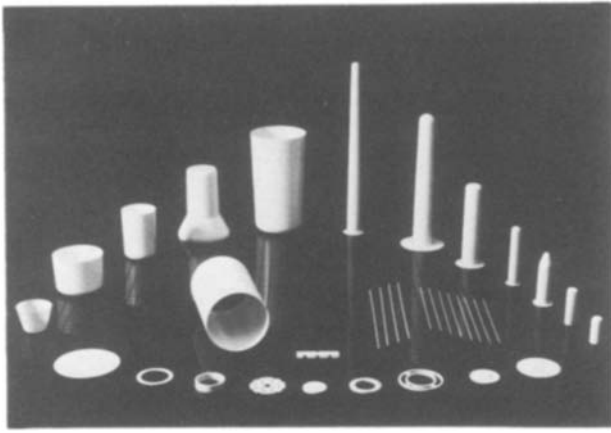


Figure 1 Articles of PBN produced by CVD process.

$$\varepsilon_r = (1 - \nu)(\alpha_r - \alpha_\theta)\Delta T \left[ \frac{1}{2} \ln \frac{r}{a} + \frac{1}{4} \left( 1 - \frac{a^2}{r^2} \right) \right] + C_1 - \frac{C_2}{r^2} \quad (4b)$$

$$\varepsilon_\theta = (1 - \nu)(\alpha_r - \alpha_\theta)\Delta T \left[ \frac{1}{2} \ln \frac{r}{a} - \frac{1}{4} \left( 1 - \frac{a^2}{r^2} \right) \right] + C_1 + \frac{C_2}{r^2} \quad (4c)$$

$$\sigma_r = \frac{E}{1 - \nu^2} \left\{ (1 - \nu)(\alpha_r - \alpha_\theta)\Delta T \left[ \frac{1 + \nu}{2} \ln \frac{r}{a} + \frac{1 - \nu}{4} \left( 1 - \frac{a^2}{r^2} \right) \right] + (1 + \nu)C_1 - \frac{1 - \nu}{r^2} C_2 - (\alpha_r + \nu\alpha_\theta)\Delta T \right\} \quad (4d)$$

$$\sigma_\theta = \frac{E}{1 - \nu^2} \left\{ (1 - \nu)(\alpha_r - \alpha_\theta)\Delta T \left[ \frac{1 + \nu}{2} \ln \frac{r}{a} - \frac{1 - \nu}{4} \left( 1 - \frac{a^2}{r^2} \right) \right] + (1 + \nu)C_1 + \frac{1 - \nu}{r^2} C_2 - (\alpha_\theta + \nu\alpha_r)\Delta T \right\} \quad (4e)$$

where  $C_1$  and  $C_2$  are constants which can be determined from the following boundary conditions.

The stress at the mandrel/crucible interface ( $r = a$ ) generated by thermal mismatch during cooling is  $P$ ,

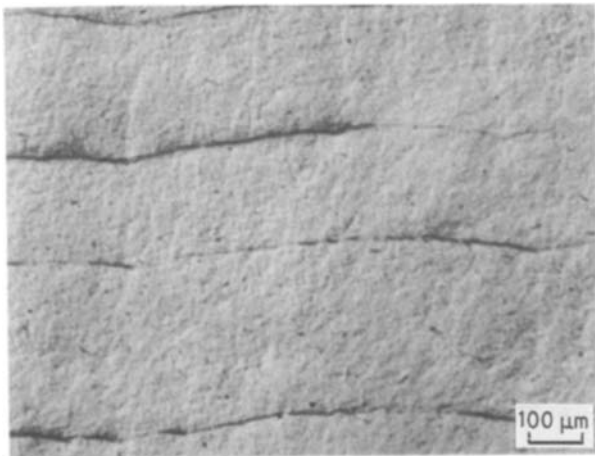


Figure 2 Delamination in PBN resulting from anisotropic contraction during cooling from its fabrication temperature.

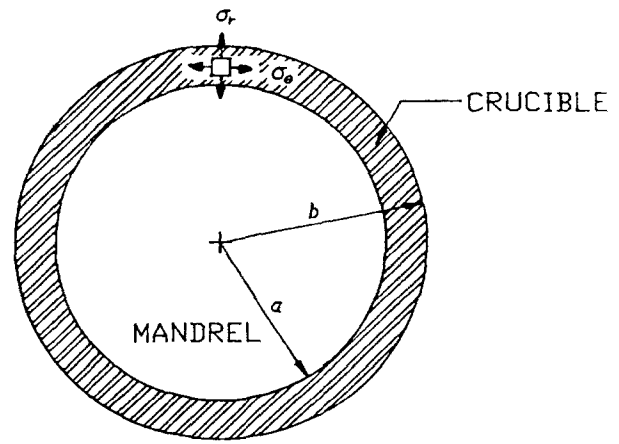


Figure 3 Schematic illustration of the PBN crucible, the mandrel and the stress components within the crucible.

such that

$$\frac{E}{1 - \nu^2} \left[ (1 + \nu)C_1 - \frac{1 - \nu}{r^2} C_2 - (\alpha_r + \nu\alpha_\theta)\Delta T \right] = P \quad (5a)$$

The outer surface ( $r = b$ ) is a free surface, such that

$$(1 - \nu)(\alpha_r - \alpha_\theta)\Delta T \left[ \frac{1 + \nu}{2} \ln \frac{b}{a} + \frac{1 - \nu}{4} \left( 1 - \frac{a^2}{b^2} \right) \right] + (1 + \nu)C_1 - \frac{1 - \nu}{b^2} C_2 - (\alpha_r + \nu\alpha_\theta)\Delta T = 0 \quad (5b)$$

Solutions of Equations 5a and b yield

$$C_1 = \frac{1}{1 + \nu} \left\{ \left[ -\frac{b^2}{b^2 - a^2} \frac{1 - \nu^2}{2} \ln \frac{b}{a} - \frac{(1 - \nu)^2}{4} \right] \times (\alpha_r - \alpha_\theta)\Delta T - \frac{a^2}{b^2 - a^2} \frac{P(1 - \nu^2)}{E} + (\alpha_r + \nu\alpha_\theta)\Delta T \right\} \quad (6a)$$

$$C_2 = -\frac{a^2 b^2}{b^2 - a^2} \left\{ (\alpha_r - \alpha_\theta)\Delta T \left[ \frac{1 + \nu}{2} \ln \frac{b}{a} + \frac{1 - \nu}{4} \left( 1 - \frac{a^2}{b^2} \right) \right] + \frac{P(1 + \nu)}{E} \right\} \quad (6b)$$

The stresses are hence

$$\sigma_r = \frac{E(\alpha_r - \alpha_\theta)\Delta T}{2} \left[ \ln \frac{r}{a} - \frac{b^2}{b^2 - a^2} \left( 1 - \frac{a^2}{r^2} \right) \ln \frac{b}{a} \right] + \frac{a^2}{b^2 - a^2} P \left( \frac{b^2}{r^2} - 1 \right) \quad (7a)$$

$$\sigma_\theta = \frac{E(\alpha_r - \alpha_\theta)\Delta T}{2} \left[ 1 + \ln \frac{r}{a} - \frac{b^2}{b^2 - a^2} \times \left( 1 + \frac{a^2}{r^2} \right) \ln \frac{b}{a} \right] - \frac{a^2}{b^2 - a^2} P \left( \frac{b^2}{r^2} + 1 \right) \quad (7b)$$

The solutions of the stresses (Equation 7) are contingent upon the magnitude of the interfacial stress,  $P$ . When the crucible separates from the mandrel during

cooling, a free surface at  $r = a$  is obtained (i.e.  $P = 0$ ), and the equations for the stresses (Equation 7) simplify accordingly

$$\sigma_r = \frac{E(\alpha_r - \alpha_\theta)\Delta T}{2} \left[ \ln \frac{r}{a} - \frac{b^2}{b^2 - a^2} \left( 1 - \frac{a^2}{r^2} \right) \ln \frac{b}{a} \right] \quad (8a)$$

$$\sigma_\theta = \frac{E(\alpha_r - \alpha_\theta)\Delta T}{2} \left[ 1 + \ln \frac{r}{a} - \frac{b^2}{b^2 - a^2} \left( 1 + \frac{a^2}{r^2} \right) \ln \frac{b}{a} \right] \quad (8b)$$

However, if the mandrel and the crucible remain in contact during cooling, the interfacial stress,  $P$ , needs to be solved from the following boundary condition.

The tangential strain of the crucible (Equation 4b) at  $r = a$  is

$$\varepsilon_\theta^c = C_1 + \frac{C_2}{a^2} \quad (9a)$$

and the tangential strain of the mandrel at  $r = a$  subjected to the interfacial stress,  $P$ , and the thermal strain is [15]

$$\varepsilon_\theta^m = \frac{1 - \nu_m}{E_m} P + \alpha_m \Delta T \quad (9b)$$

where  $E_m$ ,  $\nu_m$  and  $\alpha_m$  are the Young's modulus, Poisson ratio and thermal expansion coefficient of the mandrel, respectively. Continuity at the interface requires

$$\varepsilon_\theta^c = \varepsilon_\theta^m \quad (10)$$

Combining Equations 9 and 10 yields

$$P = \left[ \frac{1 - \nu_m}{E_m} + \frac{1}{E} \left( \nu + \frac{b^2 + a^2}{b^2 - a^2} \right) \right]^{-1} \times \left\{ (\alpha_\theta - \alpha_r) \left[ \frac{b^2}{b^2 - a^2} \ln \frac{b}{a} + \frac{1 - \nu}{2(1 + \nu)} \right] + \frac{\alpha_r + \nu\alpha_\theta}{1 + \nu} - \alpha_m \right\} \Delta T \quad (11)$$

The stresses can then be obtained by substitution of the interfacial stress (Equation 11) into Equation 7.

It is noted that, the total strains (Equation 2) in the crucible during cooling depend on the residual stresses (Equation 7). Nevertheless, the effective thermal expansion coefficients,  $\bar{\alpha}_r$  and  $\bar{\alpha}_\theta$ , can be defined:

$$\bar{\alpha}_r(r) = \varepsilon_r(r)/\Delta T \quad (12a)$$

$$\bar{\alpha}_\theta(r) = \varepsilon_\theta(r)/\Delta T \quad (12b)$$

such that the total strains (Equation 2) can be treated as stress-free strains and the material will respond with the effective thermal expansion coefficients (given by Equation 12) during cooling. In the case of  $P = 0$ , the effective thermal expansion coefficients are:

$$\bar{\alpha}_r(r) = \alpha_r + \frac{\alpha_r - \alpha_\theta}{2} \left\{ (1 - \nu) \ln \frac{r}{a} - \frac{b^2}{b^2 - a^2} \right. \\ \left. \times \left[ 1 - \nu - \frac{a^2}{r^2} (1 + \nu) \right] \ln \frac{b}{a} - \nu \right\} \quad (13a)$$

$$\bar{\alpha}_\theta(r) = \alpha_\theta + \frac{\alpha_r - \alpha_\theta}{2} \left\{ (1 - \nu) \ln \frac{r}{a} - \frac{b^2}{b^2 - a^2} \right. \\ \left. \times \left[ 1 - \nu + \frac{a^2}{r^2} (1 + \nu) \right] \ln \frac{b}{a} + 1 \right\} \quad (13b)$$

Also, the displacement of the inner surface of the crucible during cooling, in the case of  $P = 0$ , is

$$u(a) = \left[ \frac{\alpha_r - \alpha_\theta}{2} \left( 1 - \frac{2b^2}{b^2 - a^2} \ln \frac{b}{a} \right) + \alpha_\theta \right] a \Delta T \quad (14)$$

It can be derived from Equation 14 that the inner surface remains stationary ( $u(a) = 0$ ) when the thermal expansion coefficient ratio of the radial to the tangential component is

$$\frac{\alpha_r}{\alpha_\theta} = 1 + \left[ 2 / \left( \frac{2b^2}{b^2 - a^2} \ln \frac{b}{a} - 1 \right) \right] \quad (15)$$

and the inner wall will shrink or expand during cooling when the ratio is lower or higher than this critical value (Equation 15).

### 3. Results

The normalized stresses as a function of relative position,  $r/a$ , in the crucible due to thermal expansion anisotropy during cooling is plotted in Fig. 4 for  $b/a = 1.2$  and  $P = 0$ . The radial stresses are zero at the inner and outer free surfaces ( $r = a$  and  $r = b$ ), and reach a maximum tension at some radial distance value between  $a$  and  $b$ . Furthermore, the tangential stress exhibits a maximum tension at the inner wall and a maximum compression at the outer wall. The maximum in the radial and tangential tensile stresses in the crucible as a function of relative wall thickness,  $(b - a)/a$ , are plotted in Fig. 5 for  $P = 0$ . The stresses

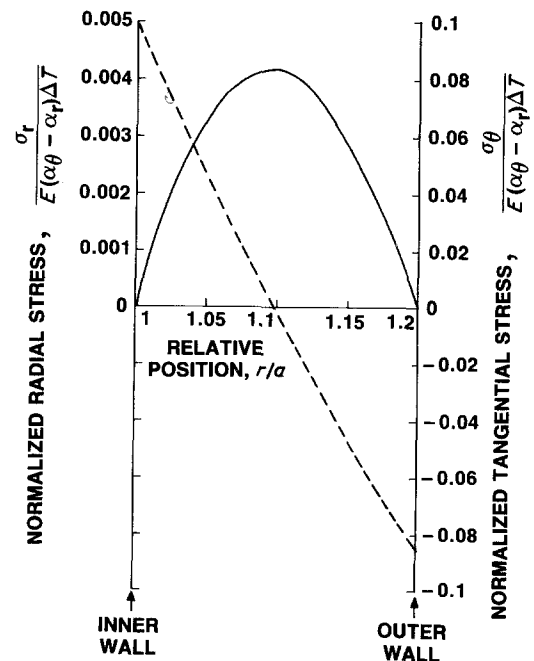


Figure 4 Normalized stress distributions as a function of the relative position within the crucible during cooling for  $b/a = 1.2$  and  $P = 0$ . (—)  $\sigma_r$ , (---)  $\sigma_\theta$ .

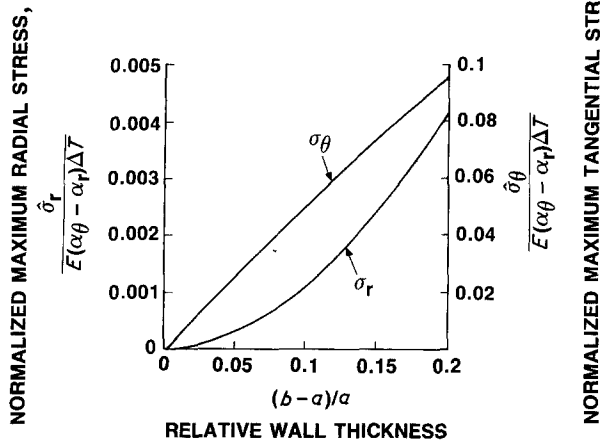


Figure 5 Normalized maximum radial and tangential stresses as a function of relative wall thickness for  $P = 0$ .

increase with increase in  $(b - a)/a$  ratio, and thus there exists a maximum wall thickness above which delamination or cracking is expected to occur.

Fig. 6 shows the effects of graphite mandrel attachment to the PBN crucible's inner wall during cooling for  $b/a = 1.2$ ,  $\Delta T = -1800^\circ\text{C}$ ,  $P \geq 0$  and the material properties listed in Table I. The radial tension in the crucible is shown to increase due to this attachment ( $P > 0$ ) which, in turn, enhances the delamination of the crucible.

The relative effective tangential thermal expansion coefficients,  $\bar{\alpha}_\theta/\alpha_\theta$ , as a function of position within the crucible for  $b/a = 1.2$  at different  $\alpha_r/\alpha_\theta$  ratios are plotted in Fig. 7. It can be visualized that  $\bar{\alpha}_\theta$  becomes smaller than  $\alpha_\theta$  in the inner wall region due to the high tangential tensile stress there (Fig. 4). Conversely,  $\bar{\alpha}_\theta$  becomes higher in the outer wall region due to the high compressive value of  $\sigma_\theta$  resulting from the enhanced

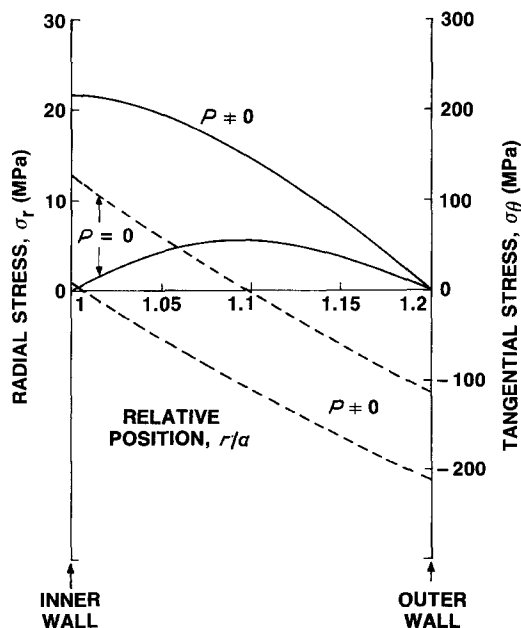


Figure 6 Normalized stress distribution within PBN for graphite mandrel attachment ( $P \neq 0$ ) and non-attachment ( $P = 0$ ) cases for  $b/a = 1.2$  and  $\Delta T = -1800^\circ\text{C}$ . (—)  $\sigma_r$ , (---)  $\sigma_\theta$ .

TABLE I Material properties of PBN and graphite

Material	$E$ (GPa)	$\nu$	$\alpha$ ( $10^{-6} \text{ }^\circ\text{C}^{-1}$ )
PBN	22	0.25	$\alpha_r = 36$ $\alpha_\theta = 2.6$
Graphite	10	0.15	3.6

shrinkage there (Fig. 4). It is also noted that while the outer wall always shrinks during cooling (positive  $\bar{\alpha}_\theta$ ), the inner wall can expand when  $\bar{\alpha}_\theta$  becomes negative at high  $\alpha_r/\alpha_\theta$  ratios (Fig. 7), where the cooling shrinkage is now overcome by the expansion generated by the residual tensile stress. Experimentally negative effective thermal expansion coefficients are observed [7, 8]. Fig. 8 shows the critical ratio of  $\alpha_r/\alpha_\theta$  as a function of  $(b - a)/a$  (Equation 15) for  $P = 0$  to achieve zero shrinkage of the inner wall. The inner wall is expected to expand during cooling when the ratio of  $\alpha_r/\alpha_\theta$  is higher than the critical value in Equation 15.

#### 4. Discussion

The present analysis reveals that residual stresses are generated in PBN crucible during cooling due to thermal contraction mismatch between the radial and the tangential directions. This results from (1) the highly oriented crystallographic texture of PBN, and (2) the very anisotropic properties of PBN. It is also reported that stresses develop due to annealing during vapour deposition of PBN at its fabrication temperature [12]. Each succeeding layer of deposited materials has less time to anneal, and thus the net effect depends upon the thermal history of deposition. Detailed analysis of these stresses due to the deposition process is beyond the scope of this article. In the absence of the stress solution due to deposition process, direct, fully quantitative comparison of the present analysis with the experimental data is not possible. However, it is hoped that the present model provides a useful basis for describing stress states and predicting cracking due to the thermal anisotropy of PBN crucibles during cooling. In addition, geometrical effects of the crucibles such as the sharp corner at the bottom of the crucible

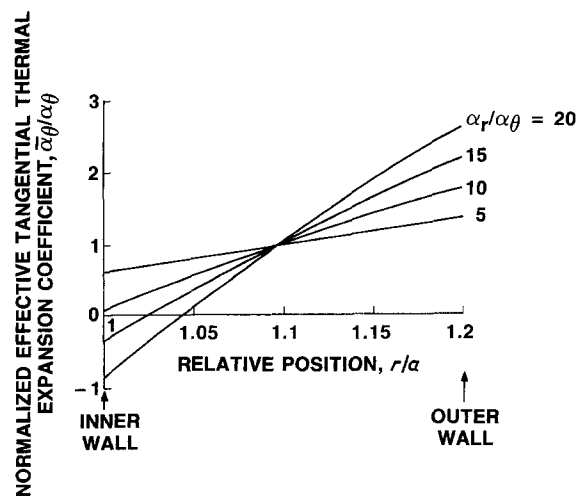


Figure 7 Normalized effective tangential thermal expansion coefficient as a function of relative position within the crucible at different ratios of  $\alpha_r/\alpha_\theta$  for  $b/a = 1.2$  and  $P = 0$ .

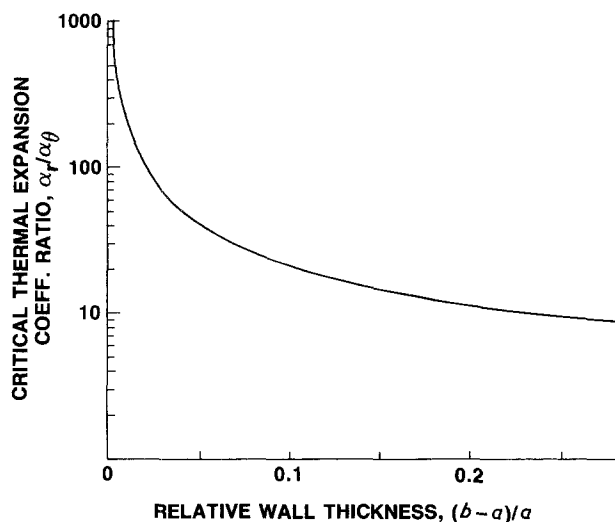


Figure 8 The critical thermal expansion coefficient ratio of  $\alpha_r/\alpha_\theta$  plotted against relative wall thickness at which the inner wall of the crucible remains stationary for  $P = 0$ .

is not considered in this study. However, the stresses are expected to increase with the increase in the curvature at the corner, resulting in detrimental characteristics.

Negative effective thermal expansion coefficients in the tangential direction obtained in this study result from the expansion generated by the residual tangential tensile stresses induced during cooling. Residual radial tensile stresses which develop in PBN crucible (Fig. 5) can be sufficient to cause cracking and delamination, which are enhanced when the interfacial stress,  $P$ , is tensile (Fig. 6). It can be visualized that when the crucible and the mandrel are attached, the interfacial stress,  $P$ , is tension when  $\alpha_m > \bar{\alpha}_\theta$ , and is compression when  $\alpha_m < \bar{\alpha}_\theta$  during cooling. Specifically, in the case of PBN with a graphite mandrel (Table I), the interfacial stress,  $P$ , is always tensile, which in turn, increases the radial tensile stress in the crucible (Fig. 6). To minimize delamination, this attachment should be avoided.

## Acknowledgement

The authors thank Drs J. H. Schneibel and P. Angelini for reviewing the manuscript. The research was sponsored by GTE Emissive Products Corp. (N. Naito) and the Division of Materials Science, US Department of Energy, under contract DE-AC05-84OR21400 with Martin Marietta Energy Systems, Inc. (C. H. Hsueh).

## References

1. M. BASCHE and D. SHIFF, *Mater. Design Engng* **2** (1964) 78.
2. G. CLERC and P. GERLACH, in "Proceedings of the 5th International Conference on Chemical Vapor Deposition", Slough, UK, September 1975, edited by J. M. Blocher Jr, H. E. Hintermann and L. H. Hall (The Electrochemical Society, Princeton, 1975) p. 777.
3. G. MALE and D. SALANOUBAT, in "Proceeding of the 7th International Conference on Chemical Vapor Deposition", Los Angeles, October 1979, edited by T. O. Sedgwick and H. Lydtin (The Electrochemical Society, Princeton, 1979) p. 391.
4. J. KOREC and M. HEYAN, *J. Crystal Growth* **60** (1982) 286.
5. M. BASCHE, US Patent 3 152 006, 6 October (1964).
6. J. M. BLOCHER Jr, M. F. BROWNING and D. M. BARRETT, in "Emergent Process Methods for High Technology Ceramics", edited by R. F. Davis, H. Palmour III and R. L. Porter (Plenum, New York, 1984) p. 299.
7. Union Carbide Corporation, "Boralloy" PBN Catalog 1987, p. 8.
8. R. S. PEASE, *Acta Crystallogr.* **5** (1952) 356.
9. K. M. TAYLOR, *Ind. Eng. Chem.* **47** (1955) 2506.
10. J. BISCOE and B. E. WARREN, *J. Appl. Phys.* **13** (1942) 364.
11. H. O. PIERSON, *J. Compos. Mater.* **9** (1975) 228.
12. C. F. POWELL, J. H. OXLEY and J. M. BLOCHER Jr, in "Vapor Deposition", (Wiley, New York, 1966) p. 659.
13. E. L. MUETTERTIES, in "The Chemistry of Boron and Its Compounds" (Wiley, New York, 1967) p. 142.
14. J. THOMAS Jr, N. E. WESTON and T. E. O'CONNOR, *J. Amer. Chem. Soc.* **84** (1963) 4619.
15. S. P. TIMOSHENKO and J. N. GOODIER, in "Theory of Elasticity" (McGraw-Hill, New York, 1951) p. 441.

Received 4 August

and accepted 22 October 1987